International Journal of Machining and Machinability of Materials

ISSN online: 1748-572X - ISSN print: 1748-5711
https://www.inderscience.com/ijmmm

Influence of wiper edge on surface integrity for end-milling of Ti-6Al-4V

Adrien Dangremont Di Crescenzo, Michel Mousseigne, Walter Rubio

DOI: 10.1504/IJMMM.2023.10054237

Article History:

Received:	22 July 2022
Last revised:	12 September 2022
Accepted:	22 September 2022
Published online:	15 March 2023

Influence of wiper edge on surface integrity for end-milling of Ti-6Al-4V

Adrien Dangremont Di Crescenzo*,
Michel Mousseigne and Walter Rubio

Institut Clément Ader,
Université Fédérale de Toulouse Midi-Pyrénées,
3 rue Caroline Aigle, Toulouse, 31400, France
Email: adrien.dangremont-di-crescenzo@univ-tlse3.fr
Email: michel.mousseigne@univ-tlse3.fr
Email: walter.rubio@univ-tlse3.fr
*Corresponding author

Abstract: The present study focuses on the process parameters influencing the surface quality of end-milled parts made of Ti-6Al-4V alloys with wiper edge insert. Part quality is understood here to mean geometric and mechanical surface criteria. The parameters involved are the cutting speed, the feed rate and the axial depth of cut. After preliminary test studies between two similar inserts, one was selected for its better performance. Then roughness and residual stresses were measured across several studies focusing on different cutting parameters. The main results of the study shows that the wiper edge plays a major role towards surface integrity and suppress the influence of feed rate and cutting speed on it. Moreover the surface integrity generated presents a roughness industrially acceptable for finishing (R_a < 0.8 μm) and compressive residual stresses that are positive towards fatigue life.

Keywords: Ti-6Al-4V; end-milling; wiper edge; roughness; residual stresses; surface integrity.

Reference to this paper should be made as follows: Di Crescenzo, A.D., Mousseigne, M. and Rubio, W. (2023) 'Influence of wiper edge on surface integrity for end-milling of Ti-6Al-4V', *Int. J. Machining and Machinability of Materials*, Vol. 25, No. 1, pp.89–110.

Biographical notes: Adrien Dangremont Di Crescenzo is a PhD student at the Clément Ader Institute, Toulouse, France. His thesis work focuses on the machining of titanium with wiper edge tools and the characterisation of the machined surface integrity.

Michel Mousseigne is an Associate Professor at the Department of Mechanical Engineering of Toulouse University France. He is a member of the Institute Clément ADER of Toulouse, France. His research interests include 3D manufacturing, surface integrity, CNC Machining.

Walter Rubio is a Full Professor at the Department of Mechanical Engineering of Toulouse University, France. He received both MS and PhD (93) in Industrial Engineering from the Toulouse University. He is a member of

the Institute Clément ADER of Toulouse. His research interests include CAD/CAM integration three- and five-axis sculptured surface manufacturing and surface integrity.

1 Introduction

Titanium alloys are difficult to machine (Ezugwu, 2005) due to their high strength at elevated temperatures, low thermal conductivity and high chemical reactivity. They are nevertheless widely used in the aeronautical industry where titanium parts are required to satisfy demanding criteria in terms of mechanical strength and safety. This is directly linked to the surface integrity generated during manufacture. Surface integrity is generally broken down into three parameters: geometric, mechanical and metallurgical. In this study, we focused on the geometric (represented by roughness) and mechanical (represented by residual stress) aspects. In the literature, various authors have observed the importance of cutting parameters such as feed rate and cutting speed on roughness. Yang and Liu (2018) observed that roughness parameters (R_a, R_t and R_z) increase with the feed rate in peripheral milling of Ti-6Al-4V. Yao et al. (2014) also noted that effect on R_a for TB6 titanium alloy in peripheral milling. For turning of Ti-6Al-4V, both Hughes et al. (2006) and Ibrahim et al. (2009) pointed out the influence of feed rate on roughness R_a. As for end milling, Shokrani et al. (2016) found the same effect with cryogenic machining of Ti-6Al-4V. Sun and Guo (2009) also highlighted the increase of roughness R_a with the increase in feed rate. Meanwhile, it appears that machining at a higher cutting speed allows roughness to be reduced. Indeed, Yang and Liu (2018) and Yao et al. (2013) described this tendency with peripheral milling of, respectively, Ti-6Al-4V and TB6 titanium alloy. Ribeiro et al. (2003) observed the same behaviour when turning Ti-6Al-4V. However, in end milling of Ti-6Al-4V, Safari et al. (2015) found that roughness decreases at first with cutting speed and then seems to stagnate at high cutting speed (300 m/min). At this point, the machining tool used showed severe wear leading to greater roughness with prolonged use. For the depth of cut, López de Lacalle et al. (2000) showed no significant influence when milling Ti-6Al-4V. However, tool wear was seen to have a significant impact on roughness. Other studies also found the negative impact of tool wear leading to greater roughness, as with Safari et al. (2015) in high-speed end milling Ti-6Al-4V and Cantero et al. (2005) who observed the same effect when drilling Ti-6Al-4V with the phenomenon accelerating as the tool life comes to an end. In turning AISI D2 steel, Davim and Figueira (2007) also reported an increase in roughness with tool wear but not in all cases. They also noted that the tool wear did not affect surface roughness. Meanwhile, contrary to the previous studies, when milling Ti-6Al-4V, López de Lacalle et al. (2000) observed an increase followed by a decrease in roughness as the tool wear increased. When turning Ti-6Al-4V, Che-Haron and Jawaid (2005) observed a positive impact on roughness with tool wear until failure of the insert. These different studies show that the relation between tool wear and roughness depends on other parameters. Ginting and Nouari (2009) showed that the tool used influences how tool wear affects roughness. Their study on end milling of Ti-6242S with two geometrically identical tools where one was coated and the other not showed that roughness decreases with tool wear for the uncoated tool while it increases for the coated one. With the appropriate lubricant, it is possible to

reduce tool wear and to improve surface roughness. The study of Singh et al. (2020) on turning Ti-6Al-4V with three lubrication strategies [dry, MQL using canola oil and nano particle-based minimum quantity lubrication (NMQL) graphene mixed in canola oil] showed the improvement of tool life and surface roughness when using NMQL and MQL over dry turning. Other studies found that lubrication have an influence over roughness (Jamil et al., 2021; Gupta et al., 2021). In a similar way to roughness, many studies have considered the evolution of residual stresses generated after machining as a function of various parameters such as feed rate, cutting speed and tool wear. For feed rate, the literature shows opposing trends. In end milling of Ti-6Al-4V, Sun and Guo (2009) observed that compressive normal residual stress decreases with the feed rate while shear residual stress increases with feed rate. In peripheral milling of Ti-6Al-4V, Yang and Liu (2018) remarked that compressive residual stress decreases with feed rate until f_z = 0.04 mm/tooth where it increases. Yao et al. (2014) found that compressive residual stress continuously increases with feed rate when high speed milling Ti-6Al-4V. The lowest feed rate was 0.08 mm/tooth, this being consistent with the observations of Yang and Liu (2018). However, in the study by Sun and Guo (2009), the range of feed rates is the same but the evolution of residual stress is opposite. Another difference between these two studies is the influence of cutting speed on residual stress. Sun and Guo (2009) found that the residual stresses were more compressive with the cutting speed up to 80 m/min, where the opposite trend emerged. Meanwhile, Yao et al. (2014) reported a steady increase in compressive residual stress over a range of 60 to 140 m/min. One explanation for these differences in residual stress trends may lie in the machining tool used and its geometry, as the machining operation conducted in both studies was similar. The influence of tool wear over residual stress is variable in the literature. Chen et al. (2004) obtained less compressive residual stress in the depth of the machined surface with tool wear during orthogonal cutting of Ti-6Al-4V. However, Hughes et al. (2006) describe more compressive residual stress in depth when turning Ti6-Al-4V. Mantle and Aspinwall (2001) also observe this effect for the maximum residual stress when end milling γ-TiAl alloy (45-2-2-0.8). The difference in behaviour of tool wear towards roughness and residual stress depends on many factors not covered in the literature. The literature has few studies investigating the role of wiper edge tool on surface integrity. A recent study of Ehsan et al. (2021) used wiper edge tool for dry high-feed milling of Ti-6Al-4V. They measured the tool life, the material removal, the roughness and the micro-hardness under high feed rate conditions. They found that the roughness increased with the depth of cut and the feed rate albeit less significantly for the feed rate than with conventional insert. In fact the wiper edge reduced the impact of higher feed rate both as it was sweeping on the surface during machining. Moreover the roughness parameter R_a was measured to be between 0.3 µm and 0.85 µm at most which is commonly accepted in industry for finishing roughness. Saleem and Mumtaz (2020) studied wiper edge used for dry face milling of Inconel 625. They found that surface roughness has been reduced at higher cutting speed while it has been increased at higher feed and depth of cut. Some other studies (Karolczak et al., 2021; Mane et al., 2017) also found that using a wiper edge insert instead of a conventional insert improve the roughness. However in the literature, relations between wiper edge insert, a non-conventional tool geometry and other aspect of surface integrity like residual stresses are not extensively studied especially on difficult-to-machine material.

The overall picture that emerges from the literature is that the influence of machining parameters on surface integrity is not fully understood especially for non-conventional

tool geometry as wiper edge insert. The objective of the present study is to provide new insights into the subject, in particular with the study of wiper edge inserts under different cutting conditions to measure roughness and surface residual stresses. To simplify matters, all tests were conducted with a new cutting edge so that tool wear will have no influence. For this purpose, two wiper edge inserts of similar macro-geometry (κ_r and insert shape) but different cutting angles were tested in order to better understand the interactions of the operating parameters in the process and the tool geometry on the surface integrity obtained. Two series of experiments focusing on the operating parameters (depth of cut, feed rate and cutting speed) were conducted to correlate their effects on surface integrity. Finally, a test study with depth of cut inferior to the cutting edge radius R_β was conducted to take advantage of the wiper edge and so generate better surface integrity.

2 Materials and experimental setup

The material used in this study was a rolled plate of Ti-6Al-4V (alloy α+β). A 5-axis machining centre (DMU 85 monoBLOCK) was used to perform the tests. For the preliminary tests, two types of inserts were selected (Figure 1). Their characteristics are shown in Table 1 (κ_r – lead angle, R_ϵ – nose radius and R_β – cutting edge radius) while the cutting geometry is provided in Table 2 in agreement with the norm ISO 3002-1:1982.

Figure 1 (a) Tool S (Sandvik RA245-032MN25-12M) (b) Tool I (Iscar S845 SNHU 1305ANR-MM) (see online version for colours)

(a) (b)

For each test performed in the present study, a new cutting edge was used with external lubrication (Vasco 6000 Blaser Swisslube). In addition, a new cutting edge has been used for each test.

Table 1 Characteristics of inserts

Insert	*Substrate*	*Coating*	κ_r	R_ϵ	R_β	*Wiper edge length*
Tool I	WC	PVD AlTiN+TiN	45°	0.8 mm	24.9 µm	3 mm
Tool S	WC	PVD TiAlN	45°	1.5 mm	24.3 µm	2.1 mm

Table 2 Cutting geometry

Insert	α_f	γ_f	α_p	γ_p
Tool I	13.3°	–1.5°	6.8°	12.8°
Tool S	18.6°	–6.2°	23.6°	16.2°

Figure 2 Representation of the six tests per plate (see online version for colours)

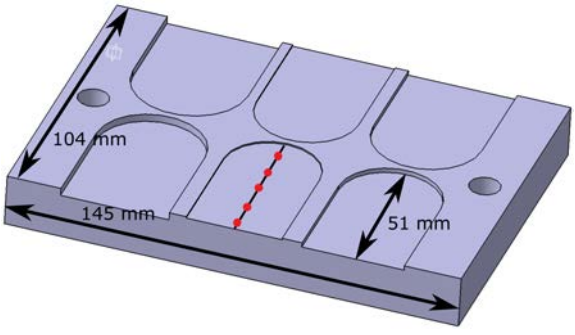

Note: The red dots represent the areas where roughness and residual stress measurements were made.

2.1 Experimental setup

Constant monitoring of the machine parameters was ensured throughout the tests. The cutting forces during machining were measured using a Kistler force plate Type 9257B and the Dynoware measurement software. Roughness was measured using the Alicona InfiniteFocusSL optical measurement system in accordance with ISO 4287-1997 and ASME B46.1-2002. The roughness profile was measured in the feed direction (Figure 2) on several points. These different measures were then used to calculate the means and standard deviations used in the study. The cutting edge of the tools was also monitored by the Alicona InfiniteFocusSL to observe the condition of the tool edge after each test. Residual stress measurements were performed by XRD on MXR's X-Raybot. This method is based on the fact that mechanical deformation induces a strain on a crystal. Compared to a stress-free crystal, the strain affects the inter-atomic spacing and this modification can be measured by diffraction (Snoha, 1996; Fitzpatrick et al., 2002). The measurements correspond to the surface residual stresses in the feed direction ($\Phi = 0°$) and were made only in that direction. Preliminary measurements on surface machined in conditions close to the preliminary test studies has been made in the feed and the transverse directions and they showed no significant difference between those two directions. Thus, the measurements in this study were made along a single direction ($\Phi = 0°$) and the number of points per surface was set at 5 (Figure 2) per test.

3 Preliminary test studies

3.1 Test parameters

The objective of this test studies was to determine the operating limits on each type of insert. The parameters chosen were based on those commonly used in industry. The cutting conditions chosen for the preliminary studies centred around values found in industry (f_z = 0.3 mm/tooth and V_C = 70 m/min). The different values for cutting speed and feed rate are shown in Figure 3. Each of these cutting conditions was applied at three different depths of cut, a_p = {0.5 mm, 1.5 mm, 2.5 mm}.

Figure 3 Representation of the five cutting conditions realised at several depth of cut (0.5 mm, 1.5 mm and 2.5 mm) (see online version for colours)

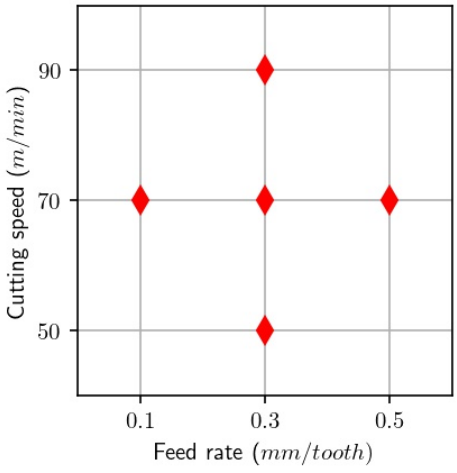

The above tests were conducted for both types of insert on Ti-6Al-4V plates of 145 mm by 104 mm with a cutting length of 51 mm. This allowed for six trials per plate (Figure 2). Test 1 was repeated four times to check repeatability of the surface generation trials. Cutting forces were measured during the milling operation using the Kistler Type 9257B dynamometer. The titanium plates were secured to the dynamometer by the holes visible on Figure 2. The forces from the dynamometer were measured on a Cartesian coordinate system while the relevant cutting forces formed part of a rotating coordinate system centred on the tool. Post-processing steps, such as filtering and changes to the coordinate system, were conducted to obtain the relevant cutting forces (Kline et al., 1982).

3.1.1 Maximum forces during experimentation

After post-processing, the maximum cutting forces for each experiment were extracted and plotted on Figures 4 and 5. For the experiments with constant feed rate (Figure 4), the evolution of tangential, radial and axial forces was seen to be similar between tool I and S. Theoretically, the cutting forces are independent of cutting speed while depth of

cut and feed rate influence the cutting forces linearly (Kaymakci et al., 2012). This can be verified for both tools and on the 3 force components at a_p = 0.5 mm. At higher a_p, the forces measured in Figure 4 show different trends. For radial forces, both for tools I and S, the forces appear to increase with the cutting speed for a_p = 1.5 mm and a_p = 2.5 mm. This evolution can be explained by the rapid tool degradation for the tests with high a_p and V_C. Indeed, rapid tool degradation tends to blunt the tool's cutting edge. Thus, the energy needed to machine a chip, the cutting force, will tend to increase. The same logic applies to the axial forces. The κ_r of 45° for both tools implies that the radial forces and axial forces are affected by the cutting edge in the same way. For the tangential forces, the results fit in with the theory. The rapid tool degradation should also influence this component. However, this effect is of minor importance as the degradation of the tool is, at the end of the test, relatively insignificant in comparison with the feed rate (f_z =0.3 mm/tooth), meaning that the tangential force needed to cut the chip depends mainly on the chip size (directly correlated to the feed rate) over degradation of the cutting edge. The same effect as for radial and axial forces should occur with a lower feed rate.

Figure 4 Maximum cutting forces for the constant feed rate (0.3 mm/tooth) tests for, (a) tool I (b) tool S (see online version for colours)

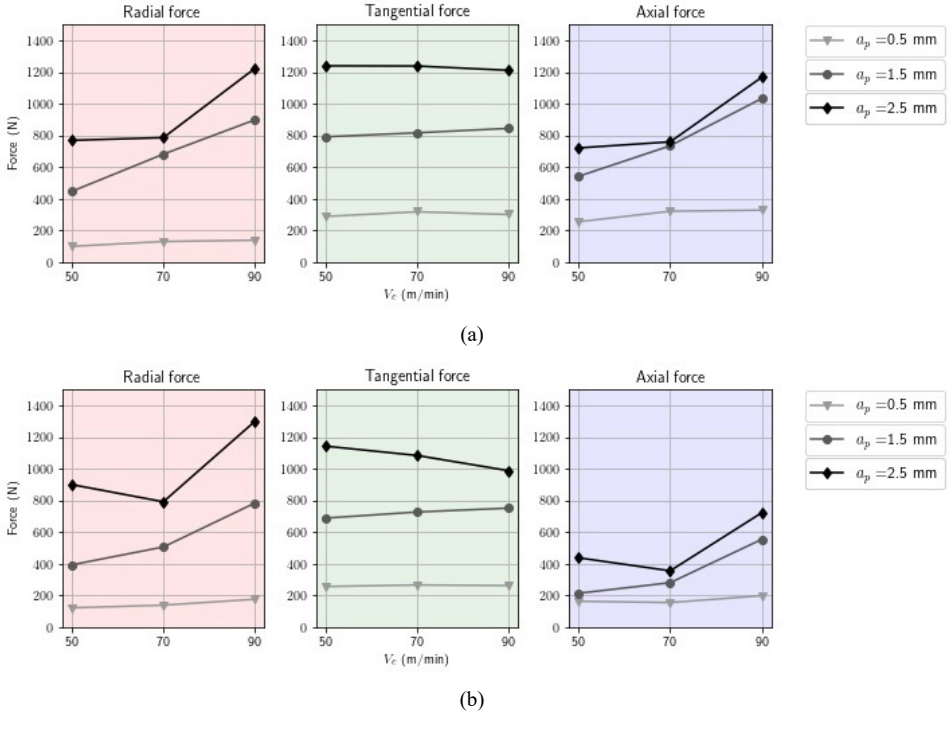

As for evolution of the cutting forces with a_p, there should be a direct proportionality. This is globally achieved for tangential forces but it is impaired by other factors such as rapid tool degradation and elastic springback. Radial and axial forces were mainly affected by tool degradation, which emerged as more significant on some tests. However, for each component, cutting forces of tool S are lower than those of tool I. This is due

to the difference in side clearance angle γ_p between tools I and S. The higher value for tool S facilitated formation of the chip, thus reducing the forces required to produce it. However, this also means that tool S is more fragile than tool I as the complementary angle of the side clearance angle γ_p and the side rake angle α_p is lower for tool S.

Figure 5 Maximum cutting forces for the fixed cutting speed (70 m/min) tests for, (a) tool I (b) tool S (see online version for colours)

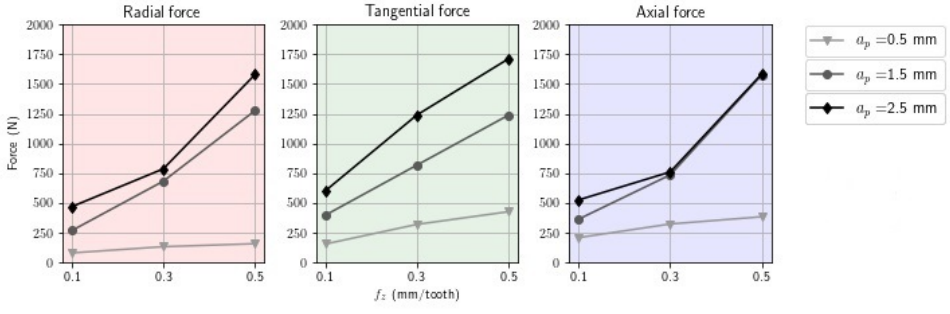

(a)

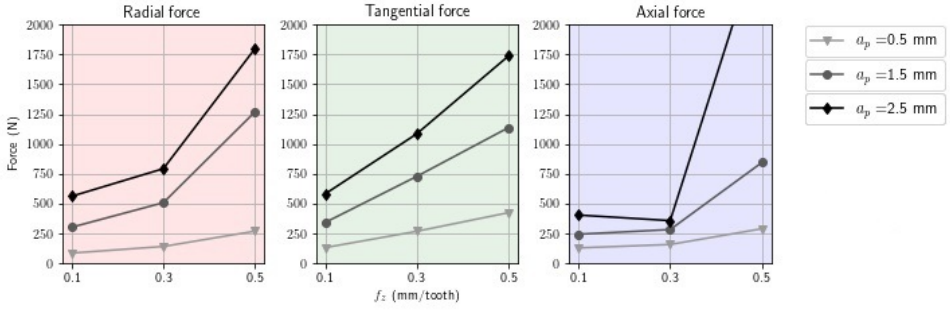

(b)

One should see a linear evolution of the feed rate in relation to the cutting forces (Figure 5). The radial and axial forces show the same trends as seen in the constant feed rate graphs (Figure 4), this departure from the theoretical linearity being related to tool degradation. Observation of the cutting edge after machining showed rapid tool degradation (Figure 6). For the tangential forces, the evolution appeared almost linear with the feed rate. For tools I and S, at f_z = 0.1 mm/tooth and a_p = 2.5 mm, the tangential forces were not linear with the subsequent measurements. In these cases, the low feed rate meant that the chip size was not greatly superior to the cutting edge used. Where intermediary feed rate points were made, they should be linear in relation to the medium and high feed rates. An incident occurred for tool S test at f_z = 0.5 mm/tooth and a_p = 2.5 mm when the insert broke during the experiment leading to extremely high axial force.

Analysis of the cutting forces for the preliminary studies highlights the presence of rapid tool degradation over several experiments. As the tool degradation modifies the cutting mechanism, deviations with theoretical relation between cutting forces and operating parameters were found in the study. This means that in many tests, the cutting

conditions were unsuitable for the inserts. To use the inserts in reliable conditions, a correlation between the operating parameters and rapid tool degradation has been made for both types of insert.

3.2 Insert degradation mapping

The preliminary studies enabled a distinction to be made between operating parameter sets with no degradation [Figures 6(a) and 6(c)] and those with rapid degradation (Figures 6(b) and 6(d)]. Overall, the four tests of Figure 6 represent a machining time between 8 and 45 seconds. The images shown below are of the same area of the cutting edge above nose radius R_ϵ for each insert.

Figure 6 Images of cutting edges of, (a) (b) tool I (c) (d) tool S, (a) $a_p = 0.5$ mm, $f_z = 0.3$ mm/tooth, $V_C = 70$ m/min (b) $a_p = 1.5$ mm, $f_z = 0.5$ mm/tooth, $V_C = 70$ m/min (c) $a_p = 1.5$ mm, $f_z = 0.1$ mm/tooth, $V_C = 70$ m/min (d) $a_p = 1.5$ mm, $f_z = 0.5$ mm/tooth, $V_C = 90$ m/min (see online version for colours)

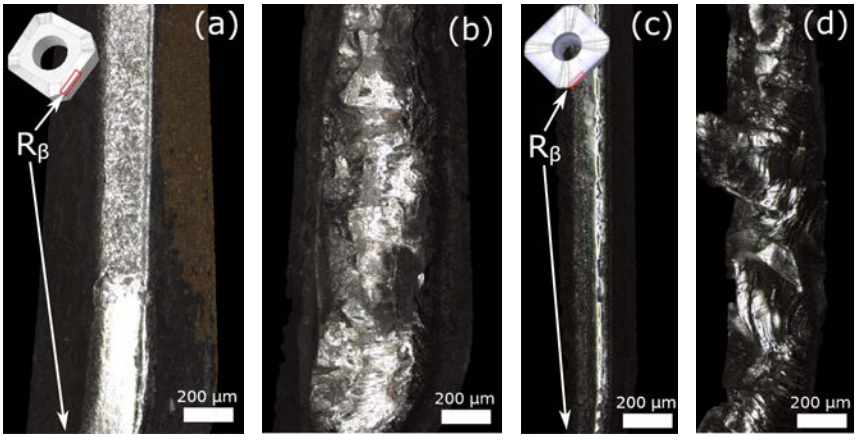

The various tests were then classified according to degradation and material removal rate. The material removal rate (in cm^3/min) was calculated from the feed rate f_z (in mm/tooth), the number of teeth Z, the cutting speed V_C (in m/min) and the depth of cut a_p (in mm):

$$D_{chip} = a_p \cdot V_c \cdot f_z \cdot Z \tag{1}$$

Comparison of degradation and material removal rate enables 3 domains delimited by iso-material removal rate curves to be identified (Figure 7): the first (shown in green on the mapping) corresponds to tests where there is no visible degradation. The second (red) corresponds to tests where degradation is heavily pronounced. The third (orange) corresponds to the intermediate domain between the two previous ones. By comparing the maps obtained (Figure 7), it can be seen that tool I can achieve higher cutting conditions than tool S before entering the degradation area. This difference between the inserts results from the cutting geometry and edge preparation. The cutting geometries

characterising tools I and S show significant differences in α_p and γ_p. Thus, the cutting edge β_p of tool S is smaller than that of tool I, making the cutter more fragile. The cutting edge β_p is defined as follows: $\alpha_p + \beta_p + \gamma_p = 90°$. With respect to cutting edge preparation (Figure 8), tool S has a small edge reinforcement and tool I has a cutting edge close to 90°. These edge preparations make both inserts globally more robust. However, combining the cutting geometry with edge preparation, it appears that tool I is more robust than tool S.

Figure 7 Degradation mapping according to cutting parameters (see online version for colours)

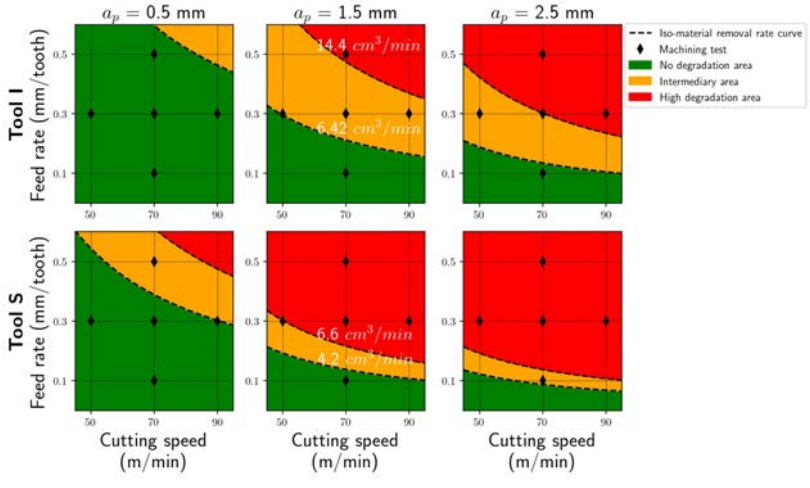

Figure 8 Cutting edge for, (a) tool S (b) tool I (see online version for colours)

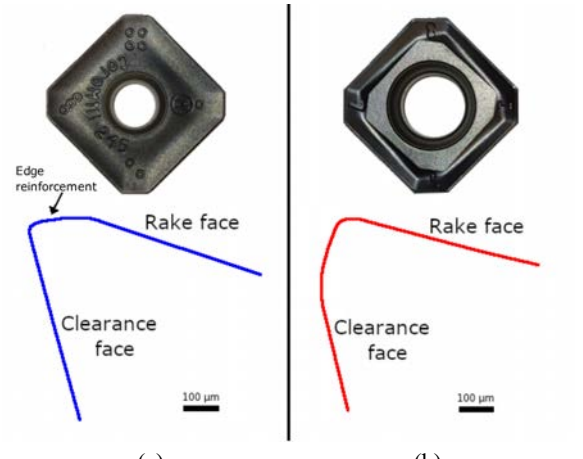

(a) (b)

Due to the limited number of tests, the iso-material removal rate curves presented here are merely indicative. Indeed, these curves were determined, for each type of insert, from a finite number of material removal rate values. However, this provides an

adequate basis for eliminating certain parameter sets and narrowing the range of cutting parameters for subsequent test studies.

In consideration of the mappings in Figure 7, tool S was excluded from the subsequent test studies. Furthermore, the 0.5 mm/tooth feed rate setting was not subsequently used due to the high tool degradation that it generated. Due to the presence of degradation observed across several tests, the depth of cut cannot be excluded from the parameters influencing surface integrity. Constant cutting speed test studies with tool I was therefore conducted to explore this issue.

4 Constant cutting speed test studies

4.1 Test parameters

The objective of these studies was to determine in greater detail the influence of the depth of cut and feed rate on surface integrity. Constant cutting speed test studies had the depth of cut and feed rate as variable parameters. The depth of cut varied from 0.5 mm to 3.0 mm by increments of 0.5 mm. These 6 tests were carried out for feed rates of 0.1 mm/tooth and 0.3 mm/tooth. For all these tests, the cutting speed was set at 50 m/min. It represented a total of 12 tests.

Figure 9 Double and single-pass areas during a test (see online version for colours)

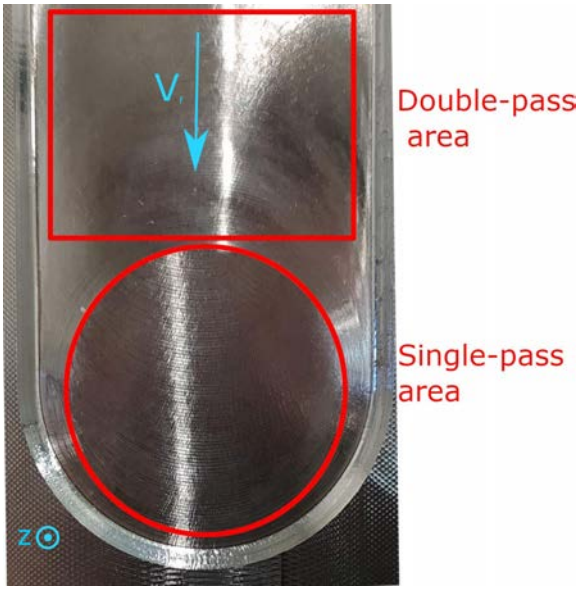

4.2 Roughness analysis

Two areas can be distinguished under the test design: the single-pass area and the double-pass area (Figure 9). During the machining, two cutting steps can be defined. When machining, the tool cut the main bulk of material in the first half of the tool rotation. This consists in the first cutting step that generates the single-pass area. On

the second half of the rotation, the tool is in contact of the surface that was already cut in the first cutting step. This friction step generates the double-pass area over the single-pass area. For each area and with each test, roughness was measured using the same protocol. The roughness profile was taken in the feed direction and analysed to measure roughness parameters such as R_a, R_t and R_z:

$$\begin{aligned} R_a &= \frac{1}{L_c}\int_0^{L_c} |z(x)|dx. \\ R_t &= |z_{\max} - z_{\min}|\,. \\ R_z &= \frac{1}{5}\left[\sum_{i=1}^{5} z_{i,\max} + \sum_{j=1}^{5} |z_{j,\min}|\right] \end{aligned} \tag{2}$$

4.2.1 Double-pass area roughness

Measurements of roughness parameters R_a and R_t are provided in Figure 10. The points correspond to the mean values and the bars to twice the standard deviation.

Figure 10 Parameters, (a) R_a (b) R_t according to depth of cut (see online version for colours)

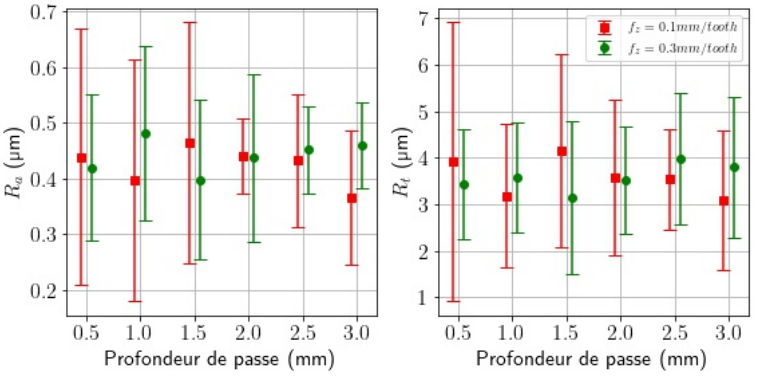

(a) (b)

The depth of cut has no significant effect on roughness. This is due to the fact that the surface where roughness is measured is generated from the bottom of the insert and therefore does not depend on the overall height of the material removed by the insert. The wiper edge generates the finished surface. The feed rate's failure to influence roughness can be explained by the tool geometry used. Indeed, tool I insert has a 3 mm wiper edge length. Depending on the feed rate chosen in the tests, the insert's wiper passes over the same area between 20 (for f_z = 0.3 mm/tooth) and 60 (for f_z = 0.1 mm/tooth) times, taking into account the passage from the front (corresponding to the cut) and from the back (corresponding to the passage of the tool over an already machined area). The high number of passes of the wiper allows the surface finish to be levelled to make it independent of the feed rate. For whatever values of depth of cut

and feed rate, the roughness is stable and the mean value remains suitable for finishing operations as the mean value of R_a = 0.44 µm is inferior to the industrial standard of 0.8 µm.

4.2.2 Single-pass area roughness

When focusing on the single-pass area, the same observations as above can be made (Figure 11). The only difference lies in the mean values for roughness. For the single-pass area, the mean values are higher (R_a = 0.6 µm and R_t = 5 µm). This shows that the passage of the tool after the initial cut improves surface quality.

Figure 11 Parameters, (a) R_a (b) R_t according to the depth of cut (see online version for colours)

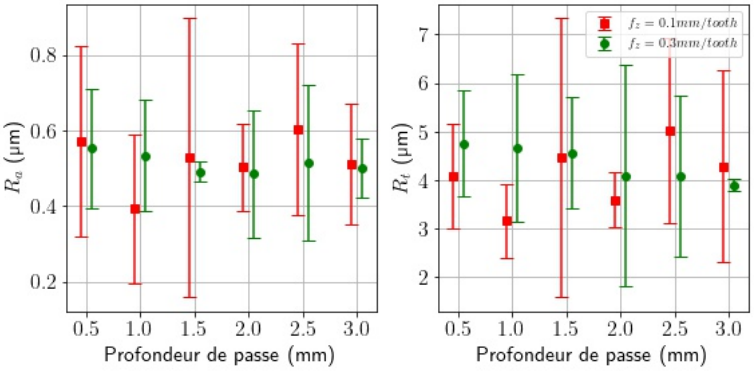

(a) (b)

4.2.3 Stress concentration factor

The stress concentration factor can be defined as follows (Arola and Ramulu, 1999):

$$K_t = 1 + n\frac{R_a}{\bar{\rho}}\frac{R_t}{R_z} \tag{3}$$

where $\bar{\rho}$ is the effective profile valley radius, R_t is the peak to valley height, R_z is the ten-point roughness, n = 1 for shear load and n = 2 for uniform tension (as chosen for the study). $\bar{\rho}$ is the average radius of the narrowest valleys (over 10 valleys). The relation between roughness and fatigue life has been made consistently in the literature. However, there are no consensus about the most relevant roughness parameter for fatigue behaviour. Some studies are using the common R_a parameter (Moussaoui et al., 2015; Jinlong et al., 2021) while other studies have argued that the stress concentration factor K_t is more representative (Yao et al., 2013; Suraratchai et al., 2008). Calculating the K_t for each test from the roughness profiles gives Figure 12 as a function of a_p.

As with the roughness parameters presented earlier, K_t does not seem to vary with the feed rate or depth of cut. The low values obtained are beneficial for fatigue behaviour as it can be seen that the stresses applied on the surface will not be strongly concentrated on a small area. Yao et al. (2013) considered the relation between the stress concentration factor and fatigue life. When milling TB6 titanium alloy, they generated

stress concentration factors ranging from 1.02 to 1.51 on different specimens and then conducted tensile fatigue tests. At K_t = 1.02, the fatigue life was improved by about 43.22% compared to the specimen at K_t = 1.51. Thus, with a mean K_t of 1.03, the fatigue life should be positively improved.

Figure 12 Stress concentration factor K_t according to the depth of cut (see online version for colours)

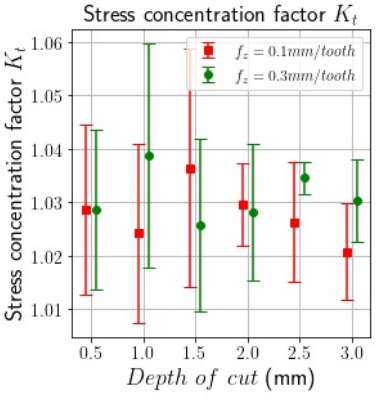

Figure 13 Residual stresses according to the depth of cut (see online version for colours)

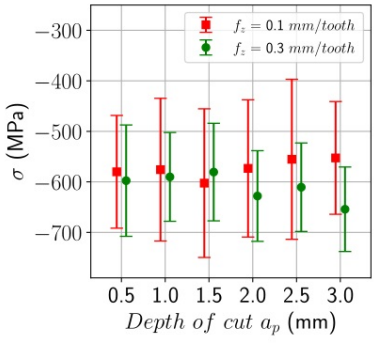

Note: The dotted black line delimits the different feed rates.

4.3 Residual stress analysis

The residual stresses measured on MXR's X-Raybot are shown in Figure 13. For these test studies, the residual stresses measured at the surface were in high compression (between –552 MPa and –654 MPa). Similarly to roughness, residual stresses were measured in the double-pass area and the single-pass area and no significant differences were noted between those two areas. The results shown below represent the mean values for residual stresses over the test. The surface residual stress measurements for the constant cutting speed test studies (Figure 13) gave residual stresses independent of the feed rate and depth of passage. The uncertainties on residual stresses came from both

the dispersion over a single test and the method of measurement in itself. The diffraction peak of Ti-6Al-4V used has intrinsically a low signal-to-noise ratio.

As with roughness, the wiper present on the insert leads to uniformity of the surface condition with respect to the cutting parameters. The non-influence of the depth of cut and of the feed rate on the residual surface stresses seems to confirm the hypothesis that surface integrity is not dependent on these two parameters. As for roughness, the wiper, through its numerous passes over the same zone, may allow the influence of the feed rate to be suppressed and thus generate similar residual stresses regardless of the latter's value.

4.4 Preliminary conclusions

The roughness and residual stress measurements show that there is no influence of the depth of cut when using a wiper edge tool, which seems to confirm that the generation of surface integrity does not depend on the depth of cut. Thus, this operating parameter can be set in order to further pursue the study of surface integrity. Furthermore, it would appear that the feed rate, for the values chosen in the tests, does not significantly influence roughness and residual stresses. The feed rate can therefore also be set with the values of the previous studies conducted. Previous work on cutting tools that do not have a wiper edge shows an influence of the feed rate and depth of pass on roughness (Sun and Guo, 2009; Ginting and Nouari, 2009) and on the residual stresses (Sun and Guo, 2009; Rao et al., 2011). This seems to corroborate the hypothesis of uniformity of the surface condition induced by the wiper regardless of feed rate and depth of cut. The final operating parameter of interest in this study is the cutting speed. Thus, a new study focusing on cutting speed was conducted.

5 Variable cutting speed test studies

5.1 Test parameters

Now, the cutting speed is the variable parameter of the test studies, ranging from 40 m/min to 120 m/min in 10 m/min increments. The feed rate was set at 0.3 mm/tooth and the depth of cut at 0.5 mm. These parameters were set in accordance with the preliminary studies where the insert showed no visible signs of degradation. This afforded greater flexibility for the cutting speed values while maintaining a reasonable removal rate. It represents a total of nine tests. The high and low limits were extended to consider areas of interest to the industry.

5.2 Roughness analysis

5.2.1 Double-pass area roughness

On the same lines as the constant cutting speed test studies, roughness measurement was performed for roughness parameters R_a and R_t. The results are shown in Figure 14. The points and error bars have the same significance and were obtained in a similar manner to the constant cutting speed studies.

Figure 14 Parameters, (a) R_a (b) R_t according to the cutting speed (see online version for colours)

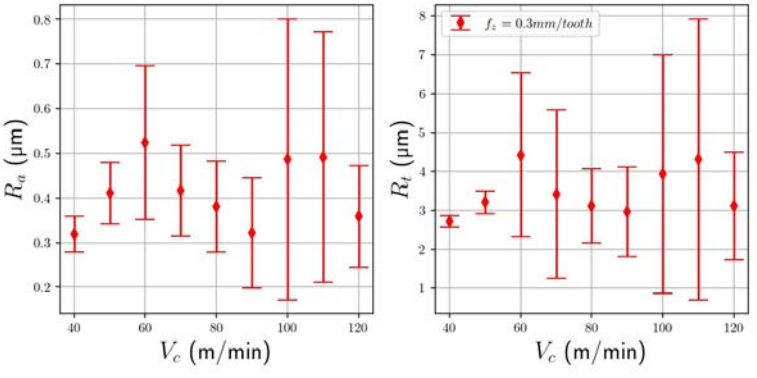

(a) (b)

Figure 15 Parameters, (a) R_a (b) R_t according to the cutting speed (see online version for colours)

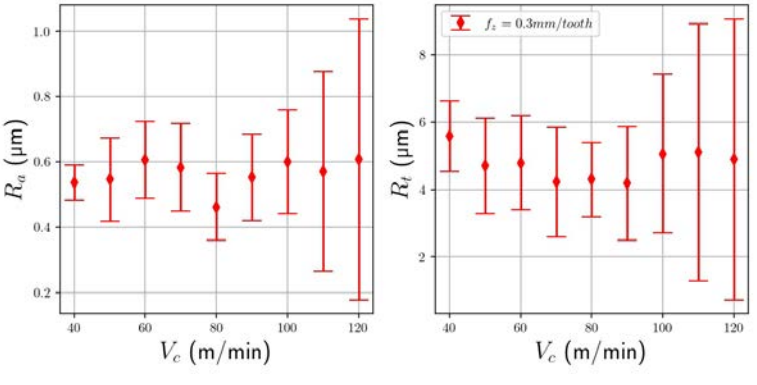

(a) (b)

Figure 16 Stress concentration factor K_t according to the cutting speed (see online version for colours)

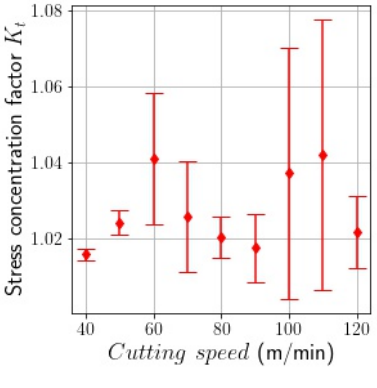

The cutting speed appears to exert an influence on roughness. It can be seen that the roughness obtained is relatively more dispersed for tests at $V_C > 50$ m/min. However, this influence should be put into perspective in view of the values obtained. Indeed, for roughness R_a, the high values remain lower than 0.8 µm, which corresponds to good finishing quality in industry. In general, the roughness values obtained are comparable to those of the constant cutting speed test studies.

5.2.2 Single-pass area roughness

The above observations also apply when focusing on the single-pass area (Figure 15). The roughness is improved on double-pass areas compared to single-pass areas while already being low in the single-pass area ($R_a < 0.8$ µm).

5.2.3 Stress concentration factor

An analysis of K_t was performed for the cutting speed studies along the lines of the constant cutting speed studies (Figure 16).

Higher cutting speeds appear to generate more surfaces showing higher stress concentration. However, the effect is still minor and will be further investigated in fatigue tests.

Figure 17 Residual stresses according to the cutting speed (see online version for colours)

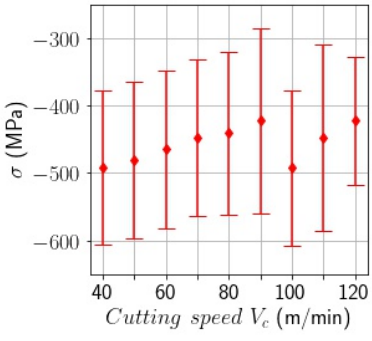

5.3 Residual stresses analysis

In this study, the measured residual stresses were still significant in compression (between –422 MPa and –492 MPa). It can be noted that the test with a_p = 0.5 mm, f_z = 0.3 mm/tooth and V_C = 50 m/min was already tested in the constant cutting speed studies. The residual stresses measured then were –597 MPa (Figure 13) as compared to –480 MPa on Figure 17. These results are not incompatible, as uncertainties remain significant (≈120 MPa). The high level of uncertainties obtained by DRX on Ti-6Al-4V has already been noted in the literature. Moussaoui et al. (2016) developed a method to measure residual stresses on Ti-6Al-4V and were faced with high-level uncertainties. These derived from the poorly shaped diffraction peak, the peak's low intensity and high background noise. All these effects contribute to increasing measurement uncertainties.

The surface residual stress measurements for the variable cutting speed test studies (Figure 17) failed to demonstrate a significant influence of the cutting speed on the generation of surface residual stresses.

For the test studies presented above, the residual stresses were similar. Thus, the generation of these stresses does not depend on the depth of cut, the feed rate or the cutting speed. The multiple passes of the wiper over the same area appear to erase the influence of the operating parameters on the residual stresses. The surface integrity generated with tool I is the same regardless of the operating parameters. As the wiper defines the final surface condition, we sought to determine whether it is possible to use the wiper to enhance surface integrity. To this purpose, we conducted another study in the microchip range.

6 Microchip range test study

6.1 Test parameters

The purpose of this test study was to study the influence of passes with the depth of cut below the R_β of the tool. Reference cutting conditions were set (V_C = 50 m/min, f_z = 0.3 mm/tooth and a_p = 0.5 mm). Its objective was to analyse the influence of the passes at very low a_p (microchip range) on surface integrity and particularly on residual stresses. The surfaces were prepared with the above reference machining conditions. The microchip tests were made immediately after preparing the surface to ensure a good precision on the depth of cut. The following cutting conditions were tested:

- one pass at a_p of 5 µm
- two passes at a_p of 5 µm
- three passes at a_p of 5 µm
- one pass at a_p of 10 µm
- two passes at a_p of 10 µm
- one pass at a_p of 20 µm.

6.2 Effects on roughness

The roughness parameters R_a and R_t were measured for each strategy (Figure 18).

For parameter R_a, lower roughness is achieved especially for strategies with a_p = 5 µm. So, it seems that a small depth of cut further improves finish in terms of roughness. For the parameter R_t, the effect was less pronounced. The various strategies contributed to decreasing Rt locally but not uniformly over the surface. This results in larger standard deviations despite the lower average R_t. The microchip strategy improved the roughness of the generated surface. However, the roughness obtained before adopting this strategy was already of good quality. In view of the values for roughness obtained here, the microchip strategy does not appear particularly relevant.

Figure 18 Parameters, (a) R_a (b) R_t for each strategy (see online version for colours)

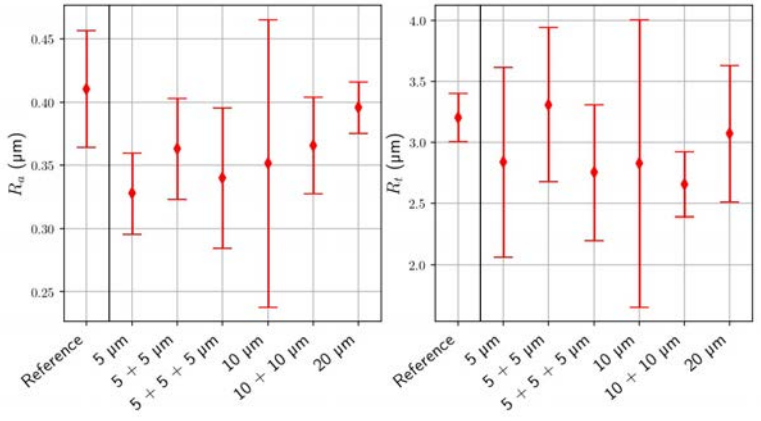

(a) (b)

6.3 *Effects on residual stresses*

As with the previous tests, the measured residual stresses were in compression. However, regardless of the strategy used, the residual stresses were similar to each other and to the reference test (Figure 19).

The microchip strategy appears to be ineffective in influencing residual surface stresses. Indeed, the different strategies applied seem to have no detrimental effect on the surface residual stresses as the values remain largely equivalent. The microchip strategy was not detrimental to either of the two aspects analysed (roughness and residual stresses). However, the only positive influence on surface integrity was seen to be in terms of roughness for one strategy (the 5 µm pass).

Figure 19 Residual stresses for each strategy (see online version for colours)

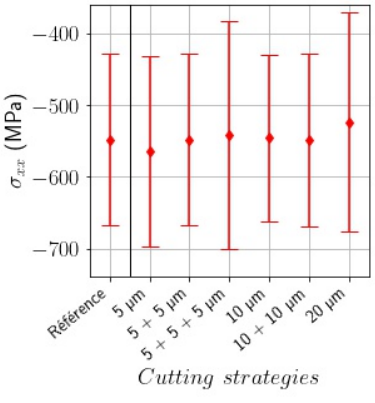

7 Conclusions

This work's main contribution relates to the influence of the wiper edge in enhancing surface integrity. It was found that the wiper plays a major role in generating a certain surface quality. The independence of the surface integrity generated from the operating parameters when using a wiper edge tool was observed for the geometrical (roughness) and mechanical (residual stresses) parameters relating to surface integrity. Thus, the tool geometry has a great influence on surface integrity. Microstructure measurements and fatigue tests will complete the study in order to consider all aspects of surface integrity. From an industrial point of view, the surface integrity generated is of good quality ($R_a < 0.8$ µm and compressive surface stress). This can help to avoid constraints on the operating parameters while guaranteeing a good quality finish. As the wiper edge generates the same surface integrity regardless of the operating parameters used, this could provide an interesting option to optimise machining time for the finishing operation using a high feed rate and/or high cutting speed.

Acknowledgements

Michel Mousseigne and Walter Rubio contributed equally to this work.

References

Arola, D. and Ramulu, M. (1999) 'An examination of the effects from surface texture on the strength of fiber reinforced plastics', *Journal of Composite Materials*, Vol. 33, No. 2, pp.102–123.

Cantero, J., Tardío, M., Canteli, J., Marcos, M. and Miguélez, M. (2005) 'Dry drilling of alloy Ti-6Al-4V', *International Journal of Machine Tools and Manufacture*, Vol. 45, No. 11, pp.1246–1255.

Che-Haron, C. and Jawaid, A. (2005) 'The effect of machining on surface integrity of titanium alloy Ti-6% Al-4% V', *Journal of Materials Processing Technology*, Vol. 166, No. 2, pp.188–192.

Chen, L., El-Wardany, T. and Harris, W. (2004) 'Modelling the effects of flank wear land and chip formation on residual stresses', *CIRP Annals*, Vol. 53, No. 1, pp.95–98.

Davim, J.P. and Figueira, L. (2007) 'Comparative evaluation of conventional and wiper ceramic tools on cutting forces, surface roughness, and tool wear in hard turning AISI D2 steel', *Proceedings of the Institution of Mechanical Engineers, Part B: Journal of Engineering Manufacture*, Vol. 221, pp.625–633.

Ehsan, S., Khan, S.A. and Rehman, M. (2021) 'Defect-free high-feed milling of Ti-6Al-4V alloy via a combination of cutting and wiper inserts', *The International Journal of Advanced Manufacturing Technology*, Vol. 114, Nos. 1–2, pp.641–653.

Ezugwu, E. (2005) 'Key improvements in the machining of difficult-to-cut aerospace superalloys', *International Journal of Machine Tools and Manufacture*, Vol. 45, Nos. 12–13, pp.1353–1367.

Fitzpatrick, M.E., Fry, A.T., Holdway, P., Kandil, F.A., Shackleton, J. and Suominen, L. (2002) *Measurement Good Practice Guide No. 52 Determination of Residual Stresses by X-ray Diffraction – Issue 2 Guide*, National Physical Laboratory, Teddington, UK.

Ginting, A. and Nouari, M. (2009) 'Surface integrity of dry machined titanium alloys', *International Journal of Machine Tools and Manufacture*, Vol. 49, Nos. 3–4, pp.325–332.

Gupta, M.K., Song, Q., Liu, Z., Sarikaya, M., Jamil, M., Mia, M., Khanna, N. and Krolczyk, G.M. (2021) 'Experimental characterisation of the performance of hybrid cryo-lubrication assisted turning of Ti-6Al-4V alloy', *Tribology International*, Vol. 153, p.106582 [online] https://doi.org/10.1016/j.triboint.2020.106582.

Hughes, J.I., Sharman, A.R.C. and Ridgway, K. (2006) 'The effect of cutting tool material and edge geometry on tool life and workpiece surface integrity', *Proceedings of the Institution of Mechanical Engineers, Part B: Journal of Engineering Manufacture*, Vol. 220, pp.93–107.

Ibrahim, G., Che-Haron, C. and Ghani, J. (2009) 'The effect of dry machining on surface integrity of titanium alloy Ti-6Al-4V ELI', *Journal of Applied Sciences*, Vol. 9, pp.121–127.

Jamil, M., Zhao, W., He, N., Gupta, M.K., Sarikaya, M., Khan, A.M., Sanjay, M.R., Siengchin, S. and Pimenov, D.Y. (2021) 'Sustainable milling of Ti-6Al-4V: a trade-off between energy efficiency, carbon emissions and machining characteristics under MQL and cryogenic environment', *Journal of Cleaner Production*, Vol. 281, p.125374 [online] https://doi.org/10.1016/j.jclepro.2020.125374.

Jinlong, W., Wenjie, P., Jing, Y., Jingsi, W., Mingchao, D. and Yuanliang, Z. (2021) 'Effect of surface roughness on the fatigue failure and evaluation of TC17 titanium alloy', *Materials Science and Technology*, Vol. 37, No. 3, pp.301–313.

Karolczak, P., Kowalski, M. and Raszka, K. (2021) 'The effect of the use of cutting zone minimum quantity lubrication and wiper geometry inserts on titanium Ti6Al4V surface quality after turning', *Tribology in Industry*, Vol. 43, No. 2, pp.321–333.

Kaymakci, M., Kilic, Z. and Altintas, Y. (2012) 'Unified cutting force model for turning, boring, drilling and milling operations', *International Journal of Machine Tools and Manufacture*, March–April, Vols. 54–55, pp.34–45.

Kline, W., DeVor, R. and Lindberg, J. (1982) 'The prediction of cutting forces in end milling with application to cornering cuts', *International Journal of Machine Tool Design and Research*, Vol. 22, No. 1, pp.7–22.

López de Lacalle, L., Pérez, J., Llorente, J. and Sánchez, J. (2000) 'Advanced cutting conditions for the milling of aeronautical alloys', *Journal of Materials Processing Technology*, Vol. 100, Nos. 1–3, pp.1–11.

Mane, P.A., Mohite, N.T., Kale, V.S. and Desai, A.A. (2017) 'Comparative assessment of standard and wiper insert on surface roughness in turning of titanium alloy (Ti-6Al-4V)', Vol. 10, No. 1, p.9.

Mantle, A. and Aspinwall, D. (2001) 'Surface integrity of a high speed milled gamma titanium aluminide', *Journal of Materials Processing Technology*, Vol. 118, Nos. 1–3, pp.143–150.

Moussaoui, K., Mousseigne, M., Senatore, J. and Chieragatti, R. (2015) 'The effect of roughness and residual stresses on fatigue life time of an alloy of titanium', *The International Journal of Advanced Manufacturing Technology*, Vol. 78, Nos. 1–4, pp.557–563.

Moussaoui, K., Segonds, S., Rubio, W. and Mousseigne, M. (2016) 'Studying the measurement by X-ray diffraction of residual stresses in Ti6Al4V titanium alloy', *Materials Science and Engineering: A*, Vol. 667, pp.340–348 [online] https://doi.org/10.1016/j.msea.2016.03.130.

Rao, B., Dandekar, C.R. and Shin, Y.C. (2011) 'An experimental and numerical study on the face milling of Ti-6Al-4V alloy: tool performance and surface integrity', *Journal of Materials Processing Technology*, Vol. 211, No. 2, pp.294–304.

Ribeiro, M., Moreira, M. and Ferreira, J. (2003) 'Optimization of titanium alloy (6Al-4V) machining', *Journal of Materials Processing Technology*, Vols. 143–144, pp.458–463 [online] https://doi.org/10.1016/S0924-0136(03)00457-6.

Safari, H., Sharif, S., Izman, S. and Jafari, H. (2015) 'Surface integrity characterization in high-speed dry end milling of Ti-6Al-4V titanium alloy', *The International Journal of Advanced Manufacturing Technology*, Vol. 78, Nos. 1–4, pp.651–657.

Saleem, M.Q. and Mumtaz, S. (2020) 'Face milling of Inconel 625 via wiper inserts: evaluation of tool life and workpiece surface integrity', *Journal of Manufacturing Processes*, Vol. 56, pp.322–336 [online] https://doi.org/10.1016/j.jmapro.2020.04.011.

Shokrani, A., Dhokia, V. and Newman, S.T. (2016) 'Investigation of the effects of cryogenic machining on surface integrity in CNC end milling of Ti-6Al-4V titanium alloy', *Journal of Manufacturing Processes*, Vol. 21, pp.172–179 [online] https://doi.org/10.1016/j.jmapro.2015.12.002.

Singh, R., Dureja, J., Dogra, M., Gupta, M.K., Mia, M. and Song, Q. (2020) 'Wear behavior of textured tools under graphene-assisted minimum quantity lubrication system in machining Ti-6Al-4V alloy', *Tribology International*, Vol. 145, p.106183 [online] https://doi.org/10.1016/j.triboint.2020.106183.

Snoha, D.J. (1996) *X-Ray Diffraction Characterization of Process-Induced Residual Stress*, US Army Research Laboratory ATTN: AMSRL-MA-I, Aberdeen Proving Ground, MD 21005-5069.

Sun, J. and Guo, Y. (2009) 'A comprehensive experimental study on surface integrity by end milling Ti-6Al-4V', *Journal of Materials Processing Technology*, Vol. 209, No. 8, pp.4036–4042.

Suraratchai, M., Limido, J., Mabru, C. and Chieragatti, R. (2008) 'Modelling the influence of machined surface roughness on the fatigue life of aluminium alloy', *International Journal of Fatigue*, Vol. 30, No. 12, pp.2119–2126.

Yang, D. and Liu, Z. (2018) 'Surface integrity generated with peripheral milling and the effect on low-cycle fatigue performance of aeronautic titanium alloy Ti-6Al-4V', *The Aeronautical Journal*, Vol. 122, No. 1248, pp.316–332.

Yao, C.F., Tan, L., Ren, J.X., Lin, Q. and Liang, Y.S. (2014) 'Surface integrity and fatigue behavior for high-speed milling Ti-10V-2Fe-3Al titanium alloy', *Journal of Failure Analysis and Prevention*, Vol. 14, pp.102–112 [online] https://doi.org/10.1016/j.apsusc.2016.06.162.

Yao, C-F., Wu, D-X., Jin, Q-C., Huang, X-C., Ren, J-X. and Zhang, D-H. (2013) 'Influence of high-speed milling parameter on 3D surface topography and fatigue behavior of TB6 titanium alloy', *Transactions of Nonferrous Metals Society of China*, Vol. 23, No. 3, pp.650–660.